Mitigation of voltage sag and voltage swell by using dynamic voltage restorer

El-Zahraa M. Mattar[1], Ekramy S. Mahmoud[2], Mohamed I. El-Sayed[1]

[1]Department of Electrical Power and Machines, Faculty of Engineering, Al-Azhar University, Cairo, Egypt
[2]Department of Electrical Power and Control, Pyramids Higher Institute for Engineering and Technology, Giza, Egypt

Article Info

ABSTRACT

Recent power quality (PQ) research shows that the most common types of power quality disturbances are voltage sags and swells in medium and low-voltage distribution grids. This paper shows how to improve two significant power quality disturbances: sags and swells voltage. To find out what effect these two PQ issues have in real life, a study case based on real nonlinear loads data from large induction motors at Beshai Company in Sadat City in Egypt is investigated. The dynamic voltage restorer (DVR) has been suggested as a solution to the voltage swell and voltage sag issues. The point of common coupling (PCC) is linked with the dynamic voltage restorer to mitigate the PQ problems that have been found. The power network, loads, and DVR may all be modeled using the MATLAB/Simulink platform. The jellyfish search optimizer (JFS) is used to get the gain settings of the proportional and integral (PI) controller for the proposed DVR. MATLAB/Simulink's results show that the proposed device is effective, reliable, and has low latency.

Corresponding Author:

El-Zahraa. M. Mattar
Department of Electrical Power and Machines, Faculty of Engineering, Al-Azhar University
Yosief Abbas Street, Cairo, Kairo, Egypt
Email: elzahraamattar24@gmail.com

1. INTRODUCTION

Electrical power should always be available because it is a necessary part of all commercial and industrial processes. Electricity quality has become not merely a technical concern but also a financial one. The four components of the power system are generating, transmitting, and power systems that supply electricity via more transmission cables to various customers at the distribution end. When the voltage at the load fluctuates, power quality in the supply network becomes crucial [1].

Power quality is becoming more essential because of the following: power electronic devices and high-tech equipment with microprocessor-based controls are more sensitive to changes in power quality. Using power electronic devices to control variable speed drives and switched modes is seen as causing a lot of electrical disturbances in the supply system, especially in service sectors like hospitals [2], [3].

Power quality problems include voltage sags, unbalance, swells, flickers, harmonic distortion, impulse transients, and interruptions. Industrial, commercial, and residential customers use a lot of power electronic devices at their installations. These devices are sensitive to problems with power quality.

Industry reliability is vulnerable, according to global studies and surveys. (long and short interruptions). Voltage sag is the biggest power quality issue in manufacturing and telecom. Power quality concerns affect power systems and load. According to Jassim *et al*. [4], harmonics also affected the current capacity of cables, transformers, and transmission lines. Al-Badri *et al*. [5] discovered that irregular loads,

such as electric furnaces, power electrical appliances, shunt capacitors, and/or inductance series resonance, are what cause power system harmonics.

Researchers have suggested reconfiguration of distribution lines, phase balancing, and rearranging between medium voltage feeds and power converter banks using a radial arrangement method to reduce voltage variation and improve distribution system voltage profiles [6]. Voltage imbalance may affect induction motor operation as illustrated in research [7]–[9]. Voltage imbalance was shown to heat windings faster than power quality issues [10] summaries the applications of power quality and standards.

According to Sousa *et al.* [11], uneven voltage supply and harmonics may coexist at the utility in case existing reasons are there, such as an induction motor with phase asymmetry or an imbalanced power network controlled by variable-frequency motors. Martiningsih *et al.* [12] instructed the Pay TV Dian Swastatika Sentosa Services (PT DSS) plant to install a dynamic voltage restorer (DVR) acting like a compensation device in sequence with the distribution cable. Proportional and integral (PI)-based DVRs can resolve power quality constraints [12].

Eltamaly *et al.* [13] developed DVR-based voltage sag mitigation and power system quality improvement. Electrical equipment has deteriorated. DVR compensates for sag/swell and adjusts voltage properly [13]. A power electronic transformer-equipped DVR reduced symmetrical and asymmetrical sags. Modern design reduces distribution line symmetrical and asymmetrical voltage sag [14].

Gabor transform (GT) [15] discussed a method and a technique to detect and classify the disturbance waveforms respectively. That it can be performed by other time-frequency analysis techniques to acquire the features. Salman *et al.* [16], two methods are used for tuning the parameters of the proportional and integral (PI) controller, trial and error and the intelligent optimal method. The utilized optimal method is the particle swarm optimization (PSO) method. The PI controller for the DVR is used to solve the power problems in research [17]. Authors used flexible alternating current transmission systems (FACTS) to mitigate power quality disturbances such as voltage fluctuations, sag, swell, and harmonics in smart grids. and compared between FACTS, (STATCOM), and unified power quality conditioner (UPQC).

This paper investigates voltage sag and voltage unbalance, which are applied on real nonlinear loads consisting of four large induction motors, and the DVR is proposed as a solution to these issues. The main contribution of this article can be summarized as follows, the real distribution system located at Beshai Company in Sadat City, Egypt is presented. Building up the DVR scheme and its application in the presented model. A proposal for jelly fish optimization algorithm to get the PI controller's gain values in DVR topology. Two power quality issues of voltage sag and voltage swell conditions are presented and power quality improvement according to mitigation of voltage sag and voltage swell. The rest of the paper is organized as: i) Section 2 presents system configuration; ii) Section 3 introduces the proposed dynamic voltage restorer with its control strategy; iii) Section 4 presents the utilized optimizer with objective function formulations; iv) Section 5 introduces the simulation results; and v) Section 6 presents the conclusion.

2. SYSTEM CONFIGURATION

The system being studied is made up of two induction motors with a 6.7 MW rating and another two induction motors with a 1.425 MW rating. They get their power from a busbar with 11 kV, which gets its power from a step-down transformer with 220/11 kV at Beshai Company in Sadat City, Egypt. As indicated in Figure 1, which is showing a MATLAB simulation of the system under study, the power goes from the transformer to the load through an underground cable that is 0.8 km long. In Table 1, the electrical equipment parameters are shown.

3. DYNAMIC VOLTAGE RESTORER

A dynamic voltage restorer (DVR) is employed to address the reported power quality issues. Between the V_g and V_L buses, a DVR structure can be found. As a power quality (PQ) conditioner, it boosts voltage, compensates for reactive power, and lessens harmonic distortion [3]. As can be seen in Figure 2(a), and Figure 2(b), the design of the filter circuit. The proposed DVR consists of three alternating current (AC)-coupled capacitors and three single-phase boosting transformers. To regulate the current, a resistance series is connected in parallel with the capacitors bank [18]. The DVR scheme's finer points are laid out in Table 2. The proposed DVR, depicted in Figure 2, includes the following parts:

- Stored energy (SE): The primary purpose of it, is to give (DVR) the actual voltage required within recompense mode [19].
- Voltage source inverter (VSI): This device converts the constant voltage from the battery to alternating voltage with the proper magnitude, phase, and frequency for injection into the transformer [20].

- Boosting transformer: It is used to make up for the voltage loss. The primary side is linked in sequence with the supply voltage (utility) and the secondary side is connected with the unit of the universal bridge.
- Filter circuit: The filter circuit consists of a resistor, inductor, and capacitor or RLC circuit which less prone to harmonic distortion in the VSI's output waveform.
- PI controller: Itis the supervisor responsible for regulating the load voltage. It does a voltage comparison between the load bus signal and the reference voltage to determine what to send to the PI controller [21].
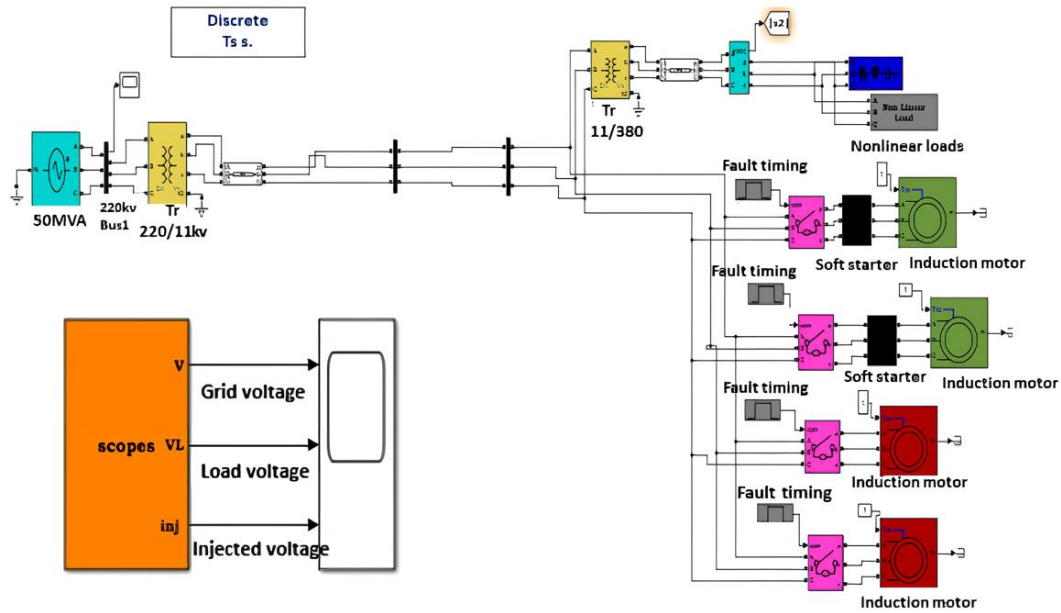
Figure 1. MATLAB-Simulink of the system under study

Table 1. The electrical element's parameters

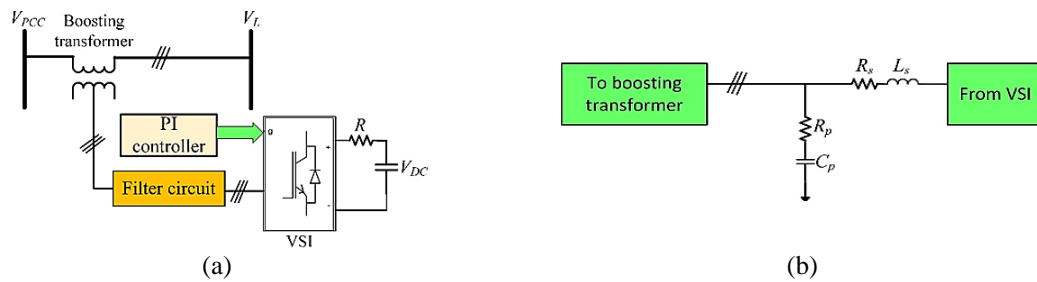| Element	Parameter
Main Grid	50 MVA, 220 kV, 50 Hz
Transformers	Tr1: 220/11kV, 50 MVA
	Tr2: 11/0.4 kV, 10 MVA
Underground cable	L=0.8 km, R=0.113 Ω/km, L=0.18 mH/km
Two induction motors (IM)	P=6700 kW, I=398 A, V=11 kV, PF=0.91
Two induction motors (IM)	P=1.425 MW, I=100 A, V=11 kV, PF=0.8
Others nonlinear loads	P=8.5 MW, Qc=5.2 Mvar, V=400 V, PF=0.85

Figure 2. DVR functional scheme model of (a) DVR scheme diagram and (b) The filter circuit design

Table 2. The DVR scheme detailed specification

Component	Value	Filter circuit component	Value
V_{DC}	7000 V	Shunt Resistance (R_p)	60 Ω
Resistant	0.2 Ω	Shunt Capacitance (C_p)	6 μF
Frequency	50 HZ	Series Inductance (L_s)	80 mH
Voltage source inverter (VIS)	Three arms, six pulses	Series resistance (R_s)	0.2 Ω
Carrier frequency	5000 Hz	The ratio of boosting transformer	1:1

3.1. Operating principle of the proposed DVR

The proposed DVR's operating principle Figure 3(a) shows a Thevenin circuit of the system being looked at, with its voltage source V_G and source impedance Z_G already chosen [22]. It gives out two packs, whose impedances are Z_L and Z_{L2}, through two feeders, V_F and V_L. The total impedance of the feeders is Z_{tot}. Kirchhoff's voltage law (KVL) is used to figure out the common bus pre-sag voltage ($V_{Pre-sag}$) and line current (I_G) while a standard DVR is running normally. The (1) and (2) demonstrate how this is done.

$$V_{pre-sag} = V_G - I_G Z_G \tag{1}$$

$$I_S = I_1 + I_2 = \frac{V_{pre-sag}}{Z_{tot} + Z_{L2}} + \frac{V_{pre-sag}}{Z_{tot} + Z_{L1}} \tag{2}$$

When a fault (F) happens on the feeder, the current that flows through it is maximum (I_{Sfault}). The (3) and (4) illustrate how much voltage is at the PCC during sag (V_{sag}).

$$V_{sag} = V_G - I_{Sfault} Z_S \tag{3}$$

$$I_{Sfault} = I_1 + I_2 = \frac{V_{sag}}{Z_{tot}} + \frac{V_{sag}}{Z_{tot} + Z_{L1}} \tag{4}$$

Figure 3(b) shows the DVR phasor diagram, when the injected voltage (V_{inj}) is low, (5) and (6) are used to estimate the magnitude and the angle of the voltage injected.

$$\left| V_{inj} \right| = \sqrt{V_L^2 + V_G^2 - 2 V_L V_G \cos(\emptyset_L - \emptyset_G)} \tag{5}$$

$$\emptyset_{inj} = \tan^{-1} \left(\frac{V_L \sin \emptyset_L - V_G \sin \emptyset_G}{V_L \cos \emptyset_L - V_G \cos \emptyset_G} \right) \tag{6}$$

The reference voltage of the three phases is summed as in (7).

$$\begin{bmatrix} V_{A_{ref}} \\ V_{B_{ref}} \\ V_{C_{ref}} \end{bmatrix} = V_{L-max} \begin{bmatrix} \sin \omega t \\ \sin \left(\omega t - \frac{2\pi}{3} \right) \\ \sin \left(\omega t + \frac{2\pi}{3} \right) \end{bmatrix} \tag{7}$$

Following that, park transformation was applied, it is transformed from three-phase abc-to-dq0 equations as shown in (8).

$$\begin{bmatrix} V_d \\ V_q \\ V_0 \end{bmatrix} = \frac{2}{3} \begin{bmatrix} \cos(\omega t) & \cos(\omega t - \frac{2\pi}{3}) & \cos(\omega t + \frac{2\pi}{3}) \\ -\sin(\omega t) & -\sin(\omega t - \frac{2\pi}{3}) & -\sin(\omega t + \frac{2\pi}{3}) \\ \frac{1}{2} & \frac{1}{2} & \frac{1}{2} \end{bmatrix} \begin{bmatrix} V_a \\ V_b \\ V_c \end{bmatrix} \tag{8}$$
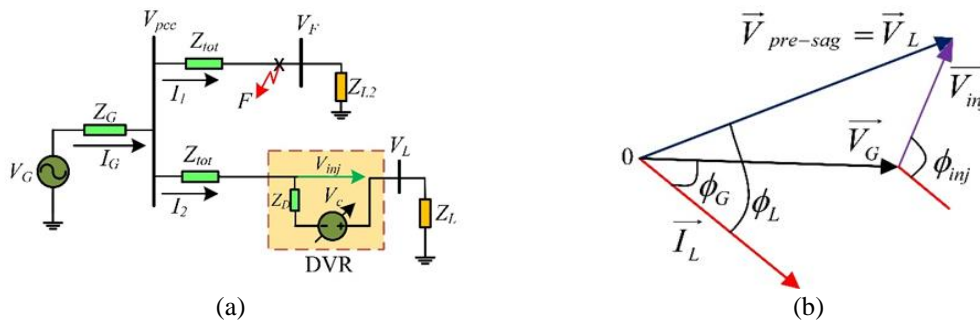

(a)   (b)

Figure 3. Operating principle of the DVR as (a) DVR Thevenin equivalent circuit
and (b) DVR phasor diagram

3.2. The suggested control scheme for DVR

Figure 3 depicts a comparison of V_L to the standard voltage; controller timing to power voltage. A detailed explanation of the controller's design is that the DVR voltages are converted into gate pulses that turn on the voltage-sensing inductor (VSI), which dampens voltage increases and compensates for decreases [23]. As shown in research [24], the proposed DVR can be operated in just five simple steps.

i) First, the disturbance type of voltage is crucial for determining the duration (beginning and ending points), depth, and stage leap [25]. Diverse load voltage techniques V_L, V_{abc}, and reference voltage V_{ref}, V_{abc} are vectorized dq0 voltage elements V_L, dq0, and it should be stressed that the primary goal of series compensation is to decrease some of the distributors' line reactance to increase load voltage. In this investigation, V_{ref} and dq0 were transformed using Park's transformation.

ii) Secondly, when converting the reference voltage (supply) and load voltage to the dq0 border, the error signal shown in (9), which is defined as a voltage amount and stage shift, will be gained.

$$|e_{t.dq0}| = \sqrt{(V_{ref.d} - V_{L.d})^2 + (V_{ref.q} - V_{L.q})^2 + (V_{ref.0} - V_{L.0})^2} \tag{9}$$

iii) Third, as explained in research [22], synchronization to the grid voltage is a key step for good management of DVR shown here. It keeps the frequency and phase of the controller's output signal in sync with an input signal that serves as a reference. So, in this work, a phase-locked loop (PLL) is employed to maintain synchronization.

iv) Fourth, the DVR control is shown in Figure 4. It is easy to understand since it is established on an error-driven of PI controller. The controller's responsibility is to minimize the grid's error signal (supply system) as much as feasible, as depicted in Figure 4. Additionally, as shown in the (10), V_c is the signal of contribution voltage in the time domain, or the PI controller at the dq0 structure of pulse-width modulation (PWM) for DVR.

$$V_{c.dq0} = K_p e_{t.dq0} + K_i \int_0^1 e_{t.dq0}\, dt \tag{10}$$

v) Fifth, The P-I controllers' output is return to the main three-phase volt V_{abc} in (11) to regulate PWM and provide the gate pulses that control of voltage source inverter, as indicated in the following diagram.

$$\begin{bmatrix} V_{c1.a} \\ V_{c1.b} \\ V_{c1.c} \end{bmatrix} = \begin{bmatrix} \sin(\omega t) & \cos(\omega t) & 1 \\ \sin(\omega t - \frac{2\pi}{3}) & \cos(\omega t - \frac{2\pi}{3}) & 1 \\ \sin(\omega t + \frac{2\pi}{3}) & \cos(\omega t + \frac{2\pi}{3}) & 1 \end{bmatrix} \begin{bmatrix} V_{c1.d} \\ V_{c1.q} \\ V_{c1.0} \end{bmatrix} \tag{11}$$
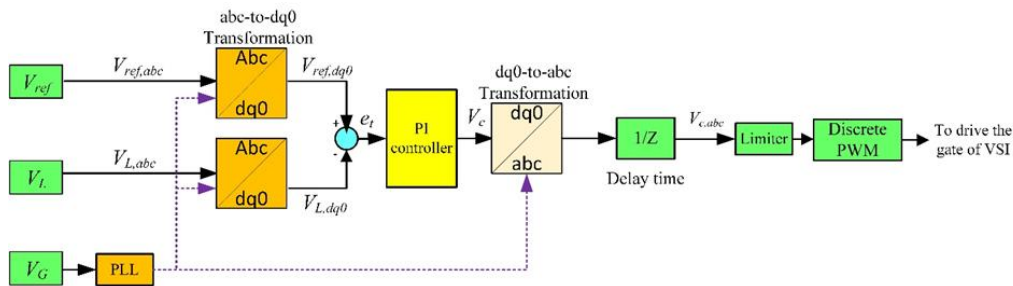

Figure 4. Scheme of control strategy proposed

4. THE OPTIMIZATION
4.1. Fitness performance

The purpose of fitness performance is to modify the PI controller gains of the suggested DVR which are described in (12).

$$minm(J) = minm(ITAE) = \int_0^\infty t|e_t|\, dt \tag{12}$$

That (J) refers to the sum error for the suggested DVR controller, ITAE acronym is for integral time absolute error. (e_t) represents the error signal. Here are some restrictions that apply to the optimisation problem.

4.2. The imposed constraints

The voltage at the second side (V_L)can only be in the range of its low and high values (13). As a result, the value cannot be lower than 0.95, also it cannot be higher than 1.05.

$$0.95 \leq V_L \leq 1.05 \tag{13}$$

The THD of the voltage (THD$_v$) of the second feeder, given by (14), should be below its maximum value ($THD_{V.max}$)as shown in (15) reported in IEEE standard 519,

$$THD_V = \frac{\sqrt{\Sigma_{h=2}^n V_h^2}}{V_1} \tag{14}$$

$$THD_V \leq THD_{V.max} \tag{15}$$

4.3. Technique for jellyfish search optimization

The jellyfish search (JFS) optimization algorithm is a new way to find the best solution. It gets its name from the way jellyfish move. They have been put into three groups. The jellyfish could first move with the current or with the rest of their group. In the meanwhile, wherever they are, areas with plenty of food attract jellyfish. The numerical fitness performance [26], [27] also reveals the quantity of food consumed. The starting population can be expressed mathematically [28].

$$X_i (t + 1) = 4P_0(1 - X_i) . 0 \leq P_0 \geq 1 \tag{16}$$

X_i (t+1) is the chaotic jellyfish equivalent. where P_0 is a value between 0 and 1 chosen at random and not equal to [0.0, 0.25, 0.75, 0.5, 1.0]. The (17) shows how to figure out the value of the temporal control function (CF), which goes from 0 to 1 [29].

$$CF (t) = \left| \left(1 - \frac{t}{T^{max}}\right) \times (2 \times r_1 - 1) \right| \tag{17}$$

t refers to the repetitions number, T$_{max}$ refers to the most repetitions that can happen, and ($r_1 - 1$)is a probability integer from 0 to 1. The (18) shows how to find out where each jellyfish was caught recently if the CF value is larger than 0.5 [28].

$$X_i (t + 1) = R \times (X^* - 3 \times R \times \mu) + X_i (t) \tag{18}$$

R refers to an integer drawn at a time from the range [0, 1], X^* represents the jellyfish's best placement within the population, and.μ represents the jellyfish population's average Based on the minimum fitness value, the best place in the population is found among the jellyfish. The fitness function, which is the amount of food, is measured for the whole jellyfish population. After putting them in order from best to worst, the first one is chosen as the best. If the CF value is less than 0.5, it can be used to calculate the fresh location of each jellyfish by using (19) to indicate the passive form and (20) to follow the active form [28].

$$X_i (t + 1) = 0.1 \times R \times (U_b - L_b)X_i (t) \tag{19}$$

$$X_i (t + 1) = \begin{cases} X_i (t) + R(X_j (t) - X_i (t)) if\ f(X_i) \geq f(X_j) \\ X_i (t) + R(X_j (t) - X_i (t)) if\ f(X_i) < f(X_j) \end{cases} \tag{20}$$

U_b and L_b stand for the control parameters' upper and lower bounds, respectively and f is a qualitative function of the amount of food in each jellyfish position. The open links for reconfiguration are related to the upper and lower bounds of the control parameters.

The (21) also describes the checking model for each jellyfish to be put back at the closest border.

$$\begin{cases} X'_{i.d} = (X_{i.d} - U_{b.d}) + L_b(d) if X_{i.d} > U_{b.d} \\ X'_{i.d} = (X_{i.d} - L_{b.d}) + U_b(d) if X_{i.d} < L_{b.d} \end{cases} \tag{21}$$

$X'_{i.d}$ shows where the ith jellyfish is located in the dth dimension. The size of the jellyfish location is the total amount of parameters of control, which are specified in (22) as the number of open links that can be changed.

$$VI = \{[O_{T1}O_{T1} … … O_{TON}]\} \tag{22}$$

(VI) is an abbreviation of the variables' independent looks, where O_T is a number of linked lines that needs to be opened the and number of them is No. As stated in the equation (23). The integer number assigned to the open connect lines should never be less than or equal to the number of linked lines, also Figure 5 shows the behavior of the jellyfish optimization technique as a flow chart. Figure 6 shows MATLAB Simulink of the system under study after connecting DVR.

$$1 \leq O_{Tj} \leq No \; j = 1.2 \ldots \ldots \ldots \ldots No \qquad (23)$$
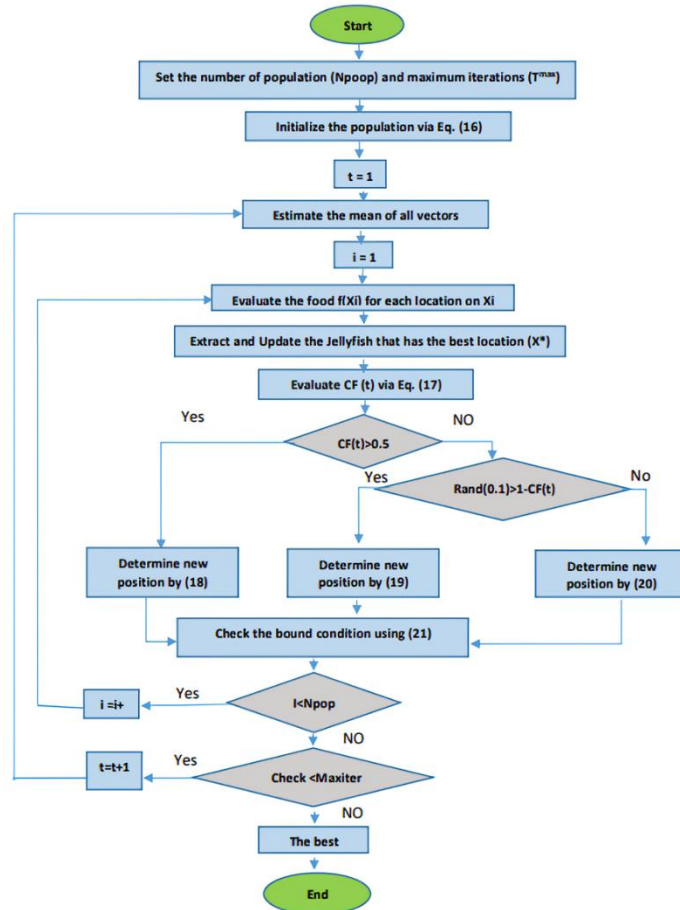
Figure 5. Main phases of the JFS
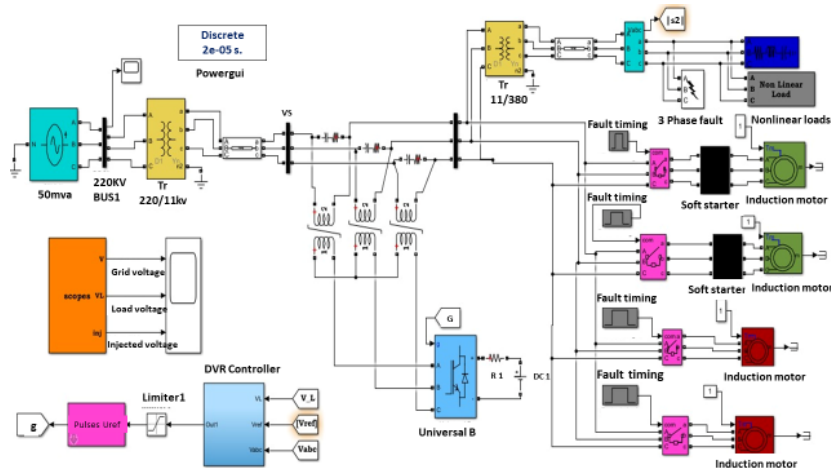
Figure 6. MATLAB Simulink of the system under study after connecting the DVR

4.4. Condition of voltage sag

At the starting mode of the actual 3-ph induction motors (three-phase), the starting time for the two motors with soft starters is between 0.1 sec and 0.2 sec. The starting time for the two motors that are connected directly online with the system is between 0.25 sec and 0.3 sec. The resulting condition is a symmetrical voltage sag(balanced). The sag at the load bus voltage is smaller than 90% to 10% if compared to the reference voltage according to IEEE. where DVR supplements the main voltage required and enhances the voltage at the load side. Figure 7(a) shows the voltage sag at the load bus when the motors start, Figure 7(b) shows the load voltage after connected DVR, and Figure 7(c) shows the compensating voltage.
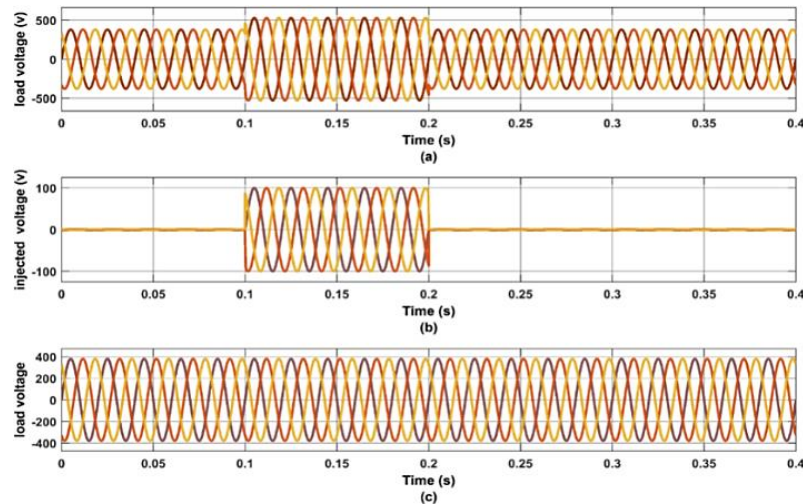
Figure 7. Results for sag condition (a) load voltage at starting, (b) load voltage after connected DVR, and (c) injected voltage by DVR

4.5. Condition of voltage swell

As a result of the three phases' switching off of various strong loads, a swell mode develops. As a result, it was assumed for this test that the voltage swell is occurring at the regular time when T=0.1 second to T=0.2 second. At the load point, the swell voltage is balanced at the three phases at a value over 120% greater than V_{ref}. During this incident, the dynamic voltage restorer corrects this problem, as shown by the simulation results. Figure 8 indicates the load bus voltage before and after the DVR-based connection. Figure 8(a) shows the voltage swell at the load bus, Figure 8(b) shows the bus load voltage after connected DVR, and Figure 8(c) shows the compensating voltage.
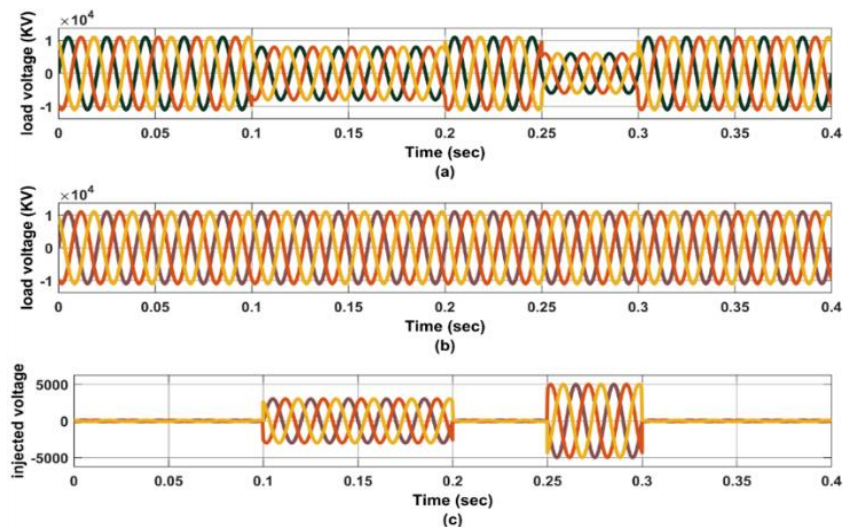

Figure 8. Results for swell condition (a) load voltage at switching off, (b) injected voltage by DVR, and (c) load voltage after connected DVR

Mitigation of voltage sag and voltage swell by using dynamic voltage restorer (El-Zahraa. M. Mattar)

4. CONCLUSION

Voltage sag and swell were presented just like two different power quality issues in this paper. Each of these power quality problems was investigated using a large load. Beshai-considered Company's load is high-power induction motors. It has been discovered that starting high-power induction motors causes sags in the voltage at the point of common coupling (PCC). Voltage swell was also resulting in the switching of heavy loads. As a series compensation device, the dynamic voltage restorer (DVR) scheme is applied. To handles issues of power quality associated with industrial loads connected to a distribution network, (DVR) is suggested to improve voltage sag and voltage swell. The jellyfish search optimizer (JFS) is utilized to get the gains values of the PI controller for the proposed DVR. The outcomes support the robustness, effectiveness, and latency of the suggested device.

REFERENCES

[1]   N. Abas, S. Dilshad, A. Khalid, M. S. Saleem, and N. Khan, "Power quality improvement using dynamic voltage restorer," *IEEE Access*, vol. 8, pp. 164325–164339, 2020, doi: 10.1109/ACCESS.2020.3022477.

[2]   A. B. Mohammed, M. A. M. Ariff, and S. N. Ramli, "Power quality improvement using dynamic voltage restorer in electrical distribution system: An overview," *Indonesian Journal of Electrical Engineering and Computer Science*, vol. 17, no. 1, pp. 86–93, 2019, doi: 10.11591/ijeecs.v17.i1.pp86-93.

[3]   Zamzami, N. Safitri, M. Arhami, and Naziruddin, "Simulation of photovoltaic station interfacing scada within transmission line," *Indonesian Journal of Electrical Engineering and Computer Science*, vol. 30, no. 3, pp. 1269–1278, 2023, doi: 10.11591/ijeecs.v30.i3.pp1269-1278.

[4]   A. H. Jassim, A. A. Hussein, and L. F. Abbas, "Study the performance of three-phase induction motor under imbalanced non-sinusoidal supply," *IOP Conference Series: Materials Science and Engineering*, vol. 1058, no. 1, p. 012035, 2021, doi: 10.1088/1757-899x/1058/1/012035.

[5]   M. Al-Badri, P. Pillay, and P. Angers, "A Novel in Situ Efficiency Estimation Algorithm for Three-Phase Induction Motors Operating with Distorted Unbalanced Voltages," *IEEE Transactions on Industry Applications*, vol. 53, no. 6, pp. 5338–5347, 2017, doi: 10.1109/TIA.2017.2728786.

[6]   P. T. Ogunboyo, R. Tiako, and I. E. Davidson, "Effectiveness of Dynamic Voltage Restorer for Unbalance Voltage Mitigation and Voltage Profile Improvement in Secondary Distribution System," *Canadian Journal of Electrical and Computer Engineering*, vol. 41, no. 2, pp. 105–115, 2022, doi: 10.1109/cjece.2018.2858841.

[7]   E. C. Quispe, I. D. López, F. J. T. E. Ferreira, and V. Sousa, "Unbalanced voltages impacts on the energy performance of induction motors," *International Journal of Electrical and Computer Engineering*, vol. 8, no. 3, pp. 1412–1422, 2018, doi: 10.11591/ijece.v8i3.pp1412-1422.

[8]   A. Adouni and A. J. M. Cardoso, "Thermal analysis of low-power three-phase induction motors operating under voltage unbalance and inter-turn short circuit faults," *Machines*, vol. 9, no. 1, pp. 1–11, 2021, doi: 10.3390/machines9010002.

[9]   P. Gnaciński, M. Peplinski, D. Hallmann, and P. Jankowski, "Induction Cage Machine Thermal Transients under Lowered Voltage Quality," *IET Electric Power Applications*, vol. 13, Mar. 2019, doi: 10.1049/iet-epa.2018.5242.

[10]   M. P. Kazmierkowski, "Reluctance Electric Machines: Design and Control [Book News]," *IEEE Industrial Electronics Magazine*, vol. 13, no. 1, pp. 61–62, Mar. 2019, doi: 10.1109/MIE.2019.2893470.

[11]   V. Sousa Santos, J. J. Cabello Eras, A. Sagastume Gutierrez, and M. J. Cabello Ulloa, "Assessment of the energy efficiency estimation methods on induction motors considering real-time monitoring," *Measurement*, vol. 136, pp. 237–247, Mar. 2019, doi: 10.1016/J.MEASUREMENT.2018.12.080.

[12]   W. Martiningsih, U. Yudho Prakoso, and H. Herudin, "Power quality improvement using dynamic voltage restorer in distribution system PT. DSS Power Plant," *MATEC Web of Conferences*, vol. 218, 2018, doi: 10.1051/matecconf/201821801003.

[13]   Y. S. and A. A. E. Ali Eltamaly, Abou-Hashema El-Sayed, "Mitigation Voltage Sag Using DVR with Power Distribution Networks for Enhancing the Power System Quality. IJEEAS Journal. Vol.1 No.2. Oct. 2018. - Google Search," no. October, 2018.

[14]   K. K. Ali, M. Talei, A. Siadatan, and S. M. H. Rad, "Power quality improvement using novel dynamic voltage restorer based on power electronic transformer," *2017 IEEE Electrical Power and Energy Conference, EPEC 2017*, vol. 2017-Octob, pp. 1–6, 2018, doi: 10.1109/EPEC.2017.8286166.

[15]   W. Tee, M. R. Yusoff, M. Faizal Yaakub, and A. R. Abdullah, "Voltage variations identification using Gabor Transform and rule-based classification method," *International Journal of Electrical and Computer Engineering*, vol. 10, no. 1, pp. 681–689, 2020, doi: 10.11591/ijece.v10i1.pp681-689.

[16]   S. S. Salman, A. T. Humod, and F. A. Hasan, "Optimum control for dynamic voltage restorer based on particle swarm optimization algorithm," *Indonesian Journal of Electrical Engineering and Computer Science*, vol. 26, no. 3, pp. 1351–1359, 2022, doi: 10.11591/ijeecs.v26.i3.pp1351-1359.

[17]   C. Science *et al.*, "Mitigating power quality disturbances in smart grid using," vol. 22, no. 3, pp. 1223–1235, 2021, doi: 10.11591/ijeecs.v22.i3.pp1223-1235.

[18]   V. Babu, K. Shafeeque Ahmed, Y. Mohamed Shuaib, and M. Manikandan, "Power Quality Enhancement Using Dynamic Voltage Restorer (DVR)-Based Predictive Space Vector Transformation (PSVT) with Proportional Resonant (PR)-Controller," *IEEE Access*, vol. 9, pp. 155380–155392, 2021, doi: 10.1109/ACCESS.2021.3129096.

[19]   R. Igual and C. Medrano, "Research challenges in real-time classification of power quality disturbances applicable to microgrids: A systematic review," *Renewable and Sustainable Energy Reviews*, vol. 132, p. 110050, 2020, doi: https://doi.org/10.1016/j.rser.2020.110050.

[20]   M. Farhadi-Kangarlu, E. Babaei, and F. Blaabjerg, "A comprehensive review of dynamic voltage restorers," *International Journal of Electrical Power & Energy Systems*, vol. 92, pp. 136–155, Nov. 2017, doi: 10.1016/J.IJEPES.2017.04.013.

[21]   A. Zobaa, P. Ribeiro, S. Abdel Aleem, and S. N. Afifi, *Energy Storage at Different Voltage Levels: Technology, integration, and market aspects*. 2018.

[22]   A. I. Omar, S. H. E. Abdel Aleem, E. E. A. El-Zahab, M. Algabalwy, and Z. M. Ali, "An improved approach for robust control of dynamic voltage restorer and power quality enhancement using grasshopper optimization algorithm," *ISA Transactions*, vol. 95, pp. 110–129, 2019, doi: https://doi.org/10.1016/j.isatra.2019.05.001.

[23] H. F. Sindi, S. Alghamdi, M. Rawa, A. I. Omar, and A. Hussain Elmetwaly, "Robust control of adaptive power quality compensator in Multi-Microgrids for power quality enhancement using puzzle optimization algorithm," *Ain Shams Engineering Journal*, vol. 14, no. 8, p. 102047, 2023, doi: https://doi.org/10.1016/j.asej.2022.102047.

[24] A. I. Omar, A. M. Sharaf, A. Shady, A. A. Mohamed, and E. Z. Essam, "Optimal Switched Compensator for Vehicle-To-Grid Battery Chargers Using Salp Optimization," *2019 21st International Middle East Power Systems Conference, MEPCON 2019 - Proceedings*, pp. 139–144, Dec. 2019, doi: 10.1109/MEPCON47431.2019.9008229.

[25] M. Awad, A. M. Ibrahim, Z. M. Alaas, A. El-Shahat, and A. I. Omar, "Design and analysis of an efficient photovoltaic energy-powered electric vehicle charging station using perturb and observe MPPT algorithm," *Frontiers in Energy Research*, vol. 10, no. August, pp. 1–22, 2022, doi: 10.3389/fenrg.2022.969482.

[26] A. H. Elmetwaly, A. A. ElDesouky, A. I. Omar, and M. Attya Saad, "Operation control, energy management, and power quality enhancement for a cluster of isolated microgrids," *Ain Shams Engineering Journal*, vol. 13, no. 5, p. 101737, 2022, doi: https://doi.org/10.1016/j.asej.2022.101737.

[27] J. L. Afonso *et al.*, "A review on power electronics technologies for power quality improvement," *Energies*, vol. 14, no. 24, 2021, doi: 10.3390/en14248585.

[28] R. Ezzeldin, H. El-Ghandour, and S. El-Aabd, "Optimal management of coastal aquifers using artificial jellyfish search algorithm," *Journal of Hydrology: Regional Studies*, vol. 41, p. 101058, 2022, doi: https://doi.org/10.1016/j.ejrh.2022.101058.

[29] R. El-Sehiemy, A. Shaheen, A. Ginidi, S. Ghoneim, M. Alharthi, and A. Elsayed, "Quasi-Reflection Jellyfish Optimizer for Optimal Power Flow in Electrical Power Systems," *Studies in Informatics and Control*, vol. 31, no. 1, pp. 49–58, 2022, doi: 10.24846/v31i1y202205.

BIOGRAPHIES OF AUTHORS

El-Zahraa. M. Mattar is bachelor's degree in engineering at Al Azhar University, Department of Electrical Power and Machines, with an overall grade of very good with honors. Currently, she is a lecturer at the Pyramids Higher Institute of Engineering, Department of Electrical Power and Control Engineering. She is interested in power system generation and control. She can be contacted at email: elzahraamahmoud2@gmail.com.

Ekramy S. Mahmoud is Ph.D. holder, doctor at the Higher Pyramids Institute, Department of Electrical Power and Control Engineering. He is specializing in electrical power quality. He can be contacted at email: ekramymahmoud619@gmail.com.

Mohammed I. El-Sayed is member of the Egyptian Electric Code Committee, an expert at the general authority of the Urban Planning in Cairo, also an associate professor at the Electrical Engineering Department., Faculty of Engineering, Al Azhar University. He received B.Sc. in electrical powers and machines field in 1997. awarded Ph.D. degree and appointed as assistant professor at the same year. He can be contacted at email: mohamedibrahimelsayed4@gmail.com.